Brain Shift Estimation in Image-Guided Neurosurgery Using 3-D Ultrasound

Marloes M. J. Letteboer*, Peter W. A. Willems, Max A. Viergever, *Member, IEEE*, and Wiro J. Niessen, *Associate Member, IEEE*

***Abstract*—Intraoperative brain deformation is one of the most important causes affecting the overall accuracy of image-guided neurosurgical procedures. One option for correcting for this deformation is to acquire three-dimensional (3-D) ultrasound data during the operation and use this data to update the information provided by the preoperatively acquired MR data.**

For 12 patients 3-D ultrasound images have been reconstructed from freehand sweeps acquired during neurosurgical procedures. Ultrasound data acquired prior to and after opening the dura, but prior to surgery, have been quantitatively compared to the preoperatively acquired MR data to estimate the rigid component of brain shift at the first stages of surgery.

Prior to opening the dura the average brain shift measured was 3.0 mm parallel to the direction of gravity, with a maximum of 7.5 mm, and 3.9 mm perpendicular to the direction of gravity, with a maximum of 8.2 mm. After opening the dura the shift increased on average 0.2 mm parallel to the direction of gravity and 1.4 mm perpendicular to the direction of gravity.

Brain shift can be detected by acquiring 3-D ultrasound data during image-guided neurosurgery. Therefore, it can be used as a basis for correcting image data and preoperative planning for intraoperative deformations.

***Index Terms*—Brain shift, computer-assisted surgery, neuronavigation, neurosurgery, 3-D ultrasound.**

I. Introduction

In neurosurgery, determining the position of lesions during interventions by navigation based on preoperatively acquired magnetic resonance imaging (MRI) data is a common approach [1], [2]. In current systems that allow for navigation on preoperative data, it is assumed that the patient's head and its content behave as a rigid body. Extrinsic features, e.g., skin markers, bone-mounted markers, and anatomical features, are used to determine the rigid body registration transformation from the coordinate system of the preoperative MR image to the coordinate system of the patient during operation. However, due to a variety of factors, including cerebrospinal fluid drainage, use of diuretics, and tumor resection [3]–[7] the brain will shift in the course of surgery with respect to the skull and, thus, with respect to the extrinsic features. This will induce an error between the actual transformation from the MR to patient coordinate system, which is nonrigid, and the rigid body registration transformation, which is used in the navigation system. This will affect the overall accuracy of image-guided neurosurgery.

Patient outcome of surgery is based on several factors, but there is increasing evidence that a more radical tumor resection is linked with a prolonged patient's survival [8], [9]. This makes it important that the tumor boundary is located as accurately as possible during surgery. This means that the error between the actual transformation from the MR to patient coordinate system and the rigid body registration transformation, induced by brain shift, has to be reduced to a minimum.

Given the potential influence on patient outcome, in recent years several attempts have been made to estimate brain shift during image-guided neurosurgery.

Several researchers [4], [5], [10], [11] have determined brain shift by comparing landmarks on the cortex, which were indicated with tracked devices, with preoperative MR image data. Mean shifts of the cortex of 5–10 mm were reported, and maximum shifts of over 20 mm. Other researchers used intraoperative MR [7], [12]–[14] and intraoperative ultrasound [3], [6] to determine brain shift, by comparing the intraoperatively acquired image data with the preoperative MR image data. With these methods not only surface shifts, but also shifts at e.g., the tumor surface and the ventricles can be estimated. Mean cortical shifts of 5–16 mm were reported, with maximum shifts of over 20 mm, and mean tumor shifts of 3–7 mm were reported, with a maximum of 15 mm.

Following the efforts to measure brain shift, an increasing number of authors has begun investigating the possibilities for correcting for brain shift during surgery. Most of the approaches rely on intraoperative imaging.

Some authors use measurements of the deformation of the cortical surface, in combination with biomechanical models of brain deformation, to estimate the influence at larger depths [15]–[19].

Since brain deformation does not only occur at the surface, but also in deeper structures of the brain, intraoperative MR or ultrasound imaging of the brain is another way to correct for deformations occurring in the course of surgery.

In the case of intraoperative MR imaging, several MR scans are acquired during surgery using an interventional MR scanner [20]–[24], which allows direct image guidance. Additionally, brain deformation can be determined and corrected by nonrigidly registering MR images acquired before surgery with MR images acquired during or after surgery, either by registration

Manuscript received October 14, 2003; revised May 25, 2004. *Asterisk indicates corresponding author.*

*M. M. J. Letteboer is with the Image Sciences Institute, University Medical Center, Heidelberglaan 100, Room Q0S.459, 3584 CX Utrecht, The Netherlands (e-mail: marloes@isi.uu.nl).

P. W. A. Willems is with the Department of Neurosurgery, University Medical Center, 3584 CX Utrecht, The Netherlands.

M. A. Viergever and W. J. Niessen are with the Image Sciences Institute, University Medical Center, 3584 CX Utrecht, The Netherlands.

Digital Object Identifier 10.1109/TBME.2004.840186

based on image content [25] or by registration based on biomechanical modeling [26]–[28]. There are some disadvantages to this approach. The interventional MR scanner limits the access of the surgeon to the operative field, special surgical tools are required and the procedure is associated with high costs.

Although intraoperative ultrasound has been used in neurosurgery since 1980 [29], it was not until 1994 that Trobaugh [30] introduced the concept of correlating intraoperative ultrasound with preoperative computed tomography (CT) or MRI during neuronavigation, by monitoring the position and orientation of the ultrasound transducer with a tracking device. Since then several research groups have developed techniques to combine two-dimensional (2-D) intraoperative ultrasound images to preoperative MR [3], [17], [31]–[36]. The disadvantages of intraoperative ultrasound are that ultrasound images suffer from relatively poor anatomical detail and excessive noise, which produces images of low resolution and signal to noise ratio.

By considering a sequence of 2-D ultrasound images, three-dimensional (3-D) ultrasound reconstructions can be made. Recently, several authors have used 3-D ultrasound for guidance during neuro-interventions [37]–[39]. A drawback of this approach, apart from limitations of intraoperative image quality, is that it can still be of clinical interest to have images from other modalities [e.g., positron emission tomography (PET), functional MRI (fMRI)] or preoperatively prepared data (e.g., segmentations, or operation plan) displayed in the image-guided surgery system.

Few researchers have addressed the combination of 3-D ultrasound with preoperative MR data for application in image-guided neurosurgery. These studies have been limited to only a few cases or phantoms. Jodicke *et al.* [40] matched preoperative MR data to intraoperative 3-D ultrasound data by segmenting and matching landmarks. They report that matching of MRI data with intraoperative 3-D ultrasound data was successful with good correspondence of landmarks. Gobbi *et al.* [41] propose interactive nonlinear registration of a preoperative MRI volume to match the intraoperative ultrasound, and demonstrate their system on a deformable phantom. Tronnier *et al.* [42] compared low-field MR imaging and 3-D-navigated ultrasonography in terms of imaging quality in lesion detection and intraoperative resection control in seven cases. Based on the preliminary results they conclude that intraoperative MR imaging remains superior to intraoperative ultrasonography in terms of resection control in gliomas surgery, however, the ultrasonography system makes a very attractive alternative. Trantakis *et al.* [43] evaluated the suitability of tracked intraoperative 3-D ultrasound for neuronavigation, and conclude that tracked US is an efficient means for controlling the validity of preoperative planning, recognition of brain shift during the intervention, replanning of the operational path due to situational changes, and controlling residual tumor resection.

The objective of this study is to show the feasibility of visualizing and measuring brain shift with intraoperatively acquired 3-D ultrasound data. Hereto, a method to intraoperatively acquire 3-D ultrasound data during image-guided surgery, using a free hand scanning technique, is introduced. A preliminary series of 12 cases is presented in which the rigid component of brain shift is determined prior to and after opening the dura. Hereto a rigid registration technique is utilized, comparing the intraoperative ultrasound data with the preoperative MR data.

TABLE I
MEDICAL DETAILS OF THE PATIENTS ON WHICH BRAIN SHIFT MEASUREMENTS ARE PERFORMED

Nr.	Age	Gender	Histology	Location
1	33	M	Glioblastoma multiforme	Right temporal lobe
2	40	M	Recurrent plexus papilloma	Posterior fossa
3	32	M	Malignent lymphoma	Left temporal lobe
4	51	M	Meningioma	Left sphenoidal ridge
5	45	M	Meningioma	Left sphenoidal ridge
6	65	M	Tentorial meningioma	Left occipital lobe
7	27	M	Astrocytoma	Left frontal lobe
8	48	M	Recurrent glioblastoma multiforme	Right frontal lobe
9	66	M	Glioblastoma	Right frontoparietal lobe
10	50	M	Anaplastic astrocytoma	Right frontal lobe
11	65	F	Glioblastoma	Left frontal lobe
12	55	M	Diffuse Astrocytoma	Left temporal lobe

II. MATERIALS AND METHODS

Brain shift measurements were performed on 12 patients, scheduled for interventions in which brain tumor tissue was resected (see Table I).

A. Preoperative MR Data Acquisition

To plan the neurosurgical procedure, images from a 1.5-tesla MRI scanner (Philips Medical Systems, Best, the Netherlands) were acquired preoperatively. All acquired images were 3-D gadolinium-enhanced, T1-weighted acquisitions, scanned with a slice thickness of 2.2 mm and reconstructed at 1.1 mm. The matrix size was 256×256, with 120–150 slices. The voxel size was $1.0 \times 1.0 \times 1.1$ mm in all cases.

These preoperative MRI datasets were transferred from the MRI scanner to the neuronavigation workstation (Stealth station TREON System with Sononav software, Medtronic Inc., Minneapolis, USA) prior to surgery.

B. Transformation From MR to Arc Coordinate System

During the neurosurgical procedure, the patient's head was rigidly fixed to the operating table with a Mayfield head clamp that immobilizes the skull. A reference arc, equipped with light emitting diodes (LEDs), was rigidly attached to the head clamp. The position of these LEDs in the operating room could be determined relative to the camera system, which is part of the navigation system.

To relate the coordinate system of the MR image acquired prior to surgery (MR coordinate system) to the coordinate system of the reference arc (arc or patient coordinate system) a rigid transformation between the two coordinate systems was determined. Prior to MR data acquisition, at least six adhesive (skin) markers were applied to the patient's head. Four or five markers were placed around the area of the craniotomy, and two markers were placed at the opposite side of the head (where they could still be tracked by a pointer that was visible for the camera system) to increase accuracy. Before the actual intervention the location of these markers in the MR data were determined by manually selecting the markers in the MR image, displayed on the image-guided surgery system. Subsequently the location of these markers in arc coordinates could by determined by pointing out the markers on the patient with a trackable pointer. A least-square fitting algorithm was used to relate the markers in MR coordinates to the markers in arc coordinates, and a rigid transformation could be calculated (1)

$$\begin{bmatrix} x_{\mathrm{arc}} \\ y_{\mathrm{arc}} \\ z_{\mathrm{arc}} \end{bmatrix} = \begin{bmatrix} T_{\mathrm{MR}\rightarrow\mathrm{arc}} \end{bmatrix} \cdot \begin{bmatrix} x_{\mathrm{MR}} \\ y_{\mathrm{MR}} \\ z_{\mathrm{MR}} \end{bmatrix}. \quad (1)$$

C. Ultrasound Data Acquisition

In order to acquire ultrasound data during the intervention, an ultrasound device (Aloka SSD-5000, with a 7.5-MHz neuroprobe, Tokyo, Japan) was connected to the neuronavigation workstation.

During an intervention at least two ultrasound sweeps were made, one prior to opening the dura and one after opening the dura but prior to surgery. During a sweep around 100 B-scans were acquired with a scanning depth of 6 to 12 cm, depending on the location of the tumor. The image size of the B-scan was 463 by 450 pixels, the voxel size depended on the scanning depth, ranging from 0.137 by 0.137 mm for a depth of 6 cm to 0.272 by 0.272 mm for a depth of 12 mm.

Before acquiring the ultrasound data, the probe was draped with a sterile surgical glove. Sterile gel was put between the glove and the probe to assure good acoustic coupling. The draped probe was put directly on the brain surface, where a fluid layer on the brain surface provided a good acoustic coupling. The sweep was made with a combination of a tilting and translational movement, acquiring a maximum of 120 B-scans within 10 s.

D. Ultrasound Calibration

Before acquiring ultrasound data, a position tracker was mounted onto the ultrasound probe, consisting of a frame with four LEDs, so the probe could be monitored continuously by the camera system. This way, the position of the tracker with respect to the reference arc was known at all times, so the tracker position in arc coordinates was known.

To relate the ultrasound image coordinates to arc coordinates, the relationship between the ultrasound image position in arc coordinates [called arcUSimage in (2)] and the tracker position in arc coordinates [called arcUStracker in (2)] needed to be established in a calibration procedure.

For the calibration procedure an ultrasound calibration phantom, containing 39 nylon wires in a tissue-equivalent material was used [44]. The wires form 13 Z-shaped patterns at 13 different depths, and were precisely located relative to the base of the phantom. The positions of the 13 Z-patterns in arc coordinates were achieved by optically tracking five LEDs, which were attached to the phantom base at known positions. When an ultrasound image of this calibration jig was acquired, the image position of each wire could be retrieved and compared to the room position of each wire, and the calibration transformation could be determined (2)

$$\begin{bmatrix} x_{\mathrm{arc}_{\mathrm{USimage}}} \\ y_{\mathrm{arc}_{\mathrm{USimage}}} \\ z_{\mathrm{arc}_{\mathrm{USimage}}} \end{bmatrix} = \begin{bmatrix} T_{\mathrm{arc}_{\mathrm{UStrac\,ker}}} \rightarrow \mathrm{arc}_{\mathrm{USimage}} \end{bmatrix} \cdot \begin{bmatrix} x_{\mathrm{arc}_{\mathrm{UStrac\,ker}}} \\ y_{\mathrm{arc}_{\mathrm{UStrac\,ker}}} \\ y_{\mathrm{arc}_{\mathrm{UStrac\,ker}}} \end{bmatrix}. \quad (2)$$

After calibration the position of the 2-D ultrasound plane could be described in arc coordinates by three vectors, one describing the position of the upper left corner of the ultrasound image (which is the origin of the ultrasound image in the ultrasound coordinate system), with respect to the origin in arc coordinates, and two vectors spanning the sides of the images (Fig. 2). From these three vectors the transformation matrix from arc coordinates to ultrasound coordinates could be determined (3)

$$\begin{bmatrix} x_{\mathrm{US}} \\ y_{\mathrm{US}} \\ z_{\mathrm{US}} \end{bmatrix} = \begin{bmatrix} T_{\mathrm{arc}\rightarrow\mathrm{US}} \end{bmatrix} \cdot \begin{bmatrix} x_{\mathrm{arc}} \\ y_{\mathrm{arc}} \\ z_{\mathrm{arc}} \end{bmatrix} \quad (3)$$

in which arc is $\mathrm{arc}_{\mathrm{USimage}}$

E. Reconstruction to a 3-D Ultrasound Volume

After surgery the 2-D ultrasound planes and their corresponding positions with respect to the reference arc were transferred to a Silicon Graphics workstation. The 2-D ultrasound planes were reconstructed to a 3-D ultrasound volume using the Stacksx software (Cambridge University Engineering Department, Cambridge, England) [45]. The Stacksx software constructs a voxel array by using bi-linear interpolation of the four nearest pixels on the closest B-scan. After reconstruction all volumes had a voxel size of $0.5 \times 0.5 \times 0.5$ mm, with a matrix size of about 256^3.

F. Relation MR to Ultrasound Coordinate Space

With the above described transformation of coordinate systems it is possible to map the preoperative MR coordinate system to the intraoperative ultrasound coordinate system, or vice versa, by simply combining the different transformations.

To relate intraoperative ultrasound images with preoperative MR images, first the position of the ultrasound image in arc coordinates has to be deduced from the tracker position, which is measured with aid of the image-guided surgery system (2), subsequently the ultrasound image coordinate system can be related

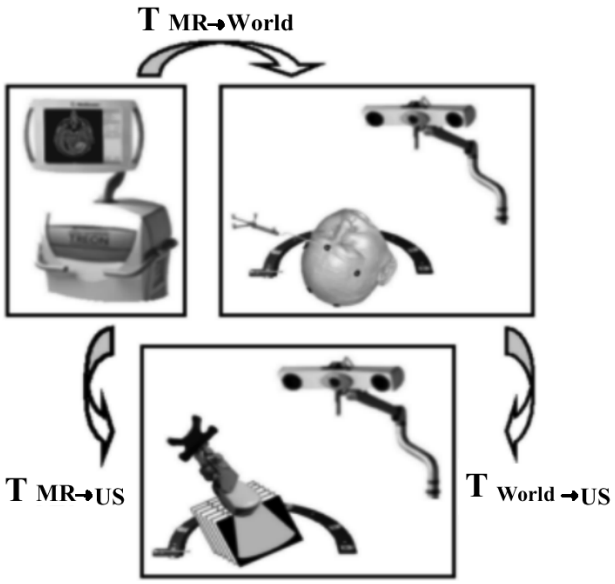

Fig. 1. Transformations between the different coordinate systems. $T_{\mathrm{MR}\rightarrow\mathrm{World}}$ gives the transformation from MR to world or arc coordinates. This transformation is established by correlating a number of adhesive skin markers, both visible in the MR data and on the patients skull, during surgery. $T_{\mathrm{World}\rightarrow\mathrm{US}}$ gives the transformation from world to ultrasound coordinates by determining the position and orientation of the ultrasound B-scan with respect to world coordinate system, related to the reference arc, with aid of the tracker device attached to the ultrasound probe. The transformation from MR to ultrasound coordinates, $T_{\mathrm{MR}\rightarrow\mathrm{US}}$, can be calculated from these two transformation matrices.

to the MR image coordinate system in the following manner (Fig. 1)

$$\begin{bmatrix} x_{\mathrm{US}} \\ y_{\mathrm{US}} \\ z_{\mathrm{US}} \end{bmatrix} = \begin{bmatrix} \\ T_{\mathrm{arc}\rightarrow\mathrm{US}} \\ \\ \end{bmatrix} \cdot \begin{bmatrix} \\ T_{\mathrm{MR}\rightarrow\mathrm{arc}} \\ \\ \end{bmatrix} \cdot \begin{bmatrix} x_{\mathrm{MR}} \\ y_{\mathrm{MR}} \\ z_{\mathrm{MR}} \end{bmatrix}. \quad (4)$$

G. Measuring Brain Shift in Patients

Brain shift will be apparent by a misregistration between the preoperative MR data, transformed to ultrasound coordinates with the aid of (4), and the ultrasound data acquired prior to and after opening of the dura. In order to estimate shift at the location of the tumor, it seems logical to outline its boundaries in both the preoperative MR and intraoperative ultrasound image. However, the entire tumor contour was not always visible in the ultrasound scans, because of a limited ultrasound beam width. Therefore, we choose to estimate the rigid component of the shift by registering the preoperatively acquired MR volume to the intraoperatively acquired US volume by a rigid registration (translation only) based on mutual information (MI). As a preprocessing step the ultrasound images are nonlinearly filtered with Perona–Malik diffusion [46] to reduce speckle noise while maintaining edges between regions of interest. The registration is performed with a manually chosen, square, region of interest around the tumor tissue, since we are primarily interested in the brain shift at the site of the tumor.

The shift is described by two components, one describing the shift parallel to the direction of gravity and one describing the shift perpendicular to gravity. Since the patient is always positioned on the operating table with the craniotomy in a, more or less, horizontal position, and the ultrasound probe is always positioned in a perpendicular position with respect to this craniotomy, the assumption is made that the y-axis (or "depth" direction) of the ultrasound volume (see Fig. 2) is parallel to gravity, and the x-, and z-axis are the perpendicular directions, where the z-axis is in the scanning direction of the ultrasound probe.

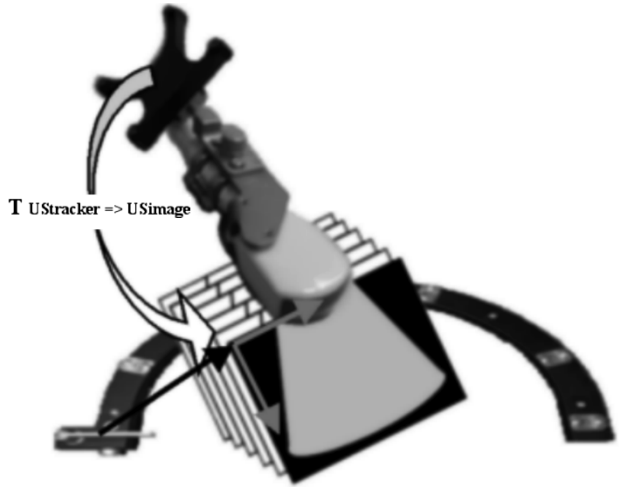

Fig. 2. Relation of ultrasound coordinate system with respect to the arc or world coordinate system. A position tracker consisting of a black frame with four LEDs mounted on it is attached to the ultrasound probe (Aloka neuroprobe, 7.5 MHz). The position of the tracker in world coordinates can be determined by the camera system. With a calibration procedure the transformation $T_{\mathrm{arc}_{\mathrm{USt\,rac\ ker}}\rightarrow\mathrm{arc}_{\mathrm{USimage}}}$ can be determined, which makes is possible to describe the position of a ultrasound B-scan in world coordinates by defining a vector from the origin of the world coordinate system to the origin of the ultrasound image, plus two vectors spanning the sides of the image (x: along the upper side of the image, y: along the 'depth' direction).

For all patients MI-based registration of the preoperative MR volume to the "pre opening dura" ultrasound volume and MI-based registration of the "pre opening dura" ultrasound volume to the "post opening dura" ultrasound volume are performed. By combining these two registrations the transformation from preoperative MR volume to "post opening dura" ultrasound volume can be determined (indirect method). This transformation can also be calculated directly by performing MI-based registration of the preoperative MR volume to the "post opening dura" ultrasound volume (direct method). By comparing the two methods the consistency of the MI-based registration method can be checked. Furthermore, to check the correctness of the registration results, tumor contours in the preoperative data are compared to tumor contours in the intraoperative data, prior to and after registration, by visual inspection and by calculating the overlap between the 3-D tumor segments. The overlap is defined as $2 \cdot (V_1 \cap V_2)/(V_1 + V_2)$, where V_1 is the volume of the tumour in the MR image and V_2 is the volume of the tumour in the ultrasound image. For the manual segmentation of these tumours, a contour around the tumour is drawn by hand in sagital, transversal, and coronal reformatted images. The datasets are examined slice by slice. After the whole dataset is examined in one orthogonal direction, it is examined again it at least one other orthogonal direction and corrections are made if necessary.

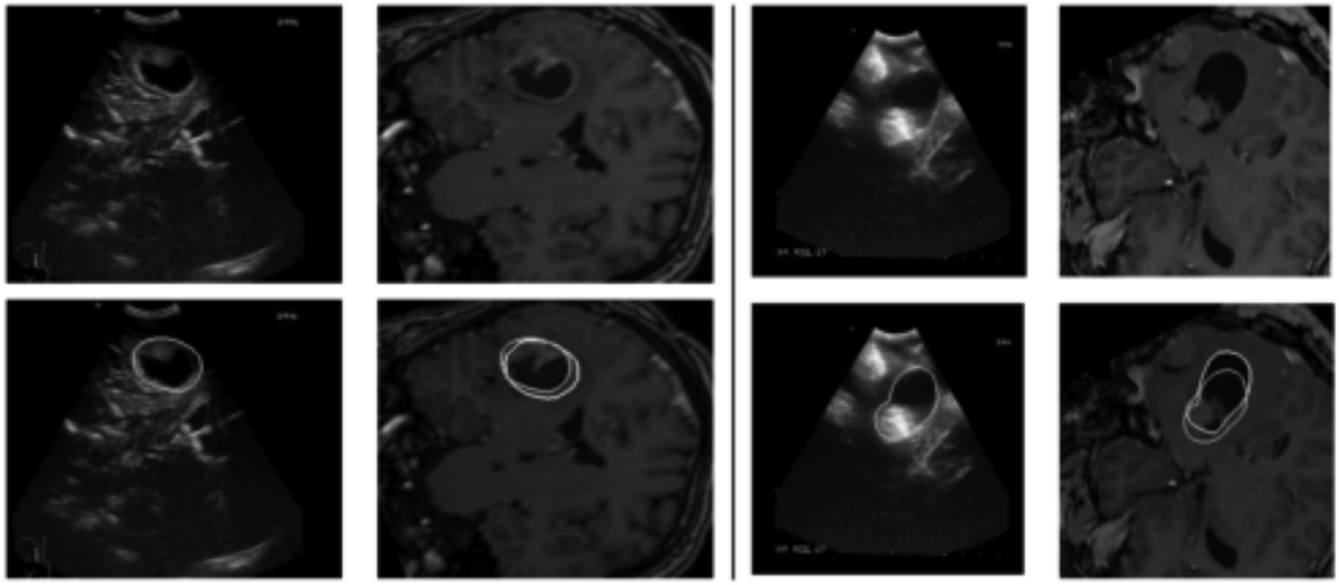

Fig. 3. Transformation of preoperative MR data to intraoperative US data with the aid of the image-guided surgery system. The figure shows the results for two patients. For each patient four images are displayed: upper left: ultrasound image, after opening the dura; upper right: MR image transformed to the intraoperative ultrasound image; bottom left: as upper left with the tumor contour projected (gray); bottom right: as upper right with the MR tumor contour (white) and the ultrasound tumor contour (gray) projected. Brain shift is apparent by comparing tumor contours in the preoperative MR and intraoperative US images.

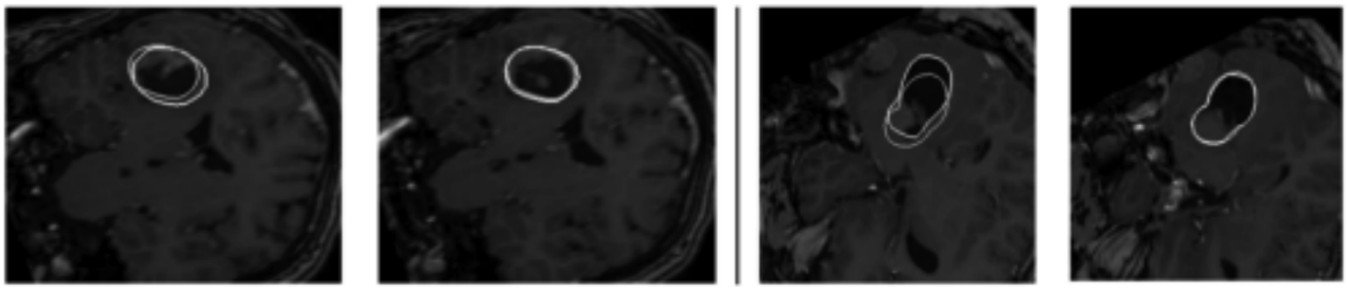

Fig. 4. MI-based registration of preoperative MR data to intraoperative US data. The figure shows the results for two patients (the same patients as in Fig. 3). For each patient two images are displayed: left: MR image, prior to registration with MR tumor contour (white) and US tumor contour (gray) projected; right: MR image, after registration with the new MR tumor contour (white) and US tumor contour (gray) projected. It can be seen that the contours overlap better after MI-based registration.

III. Results

In Table I, the clinical details of the 12 patients are summarized. The histology and location of the tumors vary significantly for the 12 cases investigated and, therefore, no general conclusions can be drawn.

For the 12 patients investigated the position of the tumor could be located well in all ultrasound scans. The margins of the tumors could be well defined in eight patients and moderately defined in four (patients 4, 5, 10, and 11). In these latter patients it was clear where the tumor was located but diffuse margins made boundary definition difficult.

As a first step, the preoperative MR images were transformed to the ultrasound coordinate system according to (4). The preoperative MR and intraoperative (3-D) ultrasound data could then be displayed in the same coordinate system. Fig. 3 shows the result of the transformation of a preoperative MR image to the intraoperative ultrasound image, for two patients. Brain shift is apparent by comparing tumor contours in the preoperative MR (white) and intraoperative ultrasound images (gray).

Next, the MR images were registered to the ultrasound image, by image registration based on MI, to measure the rigid component of brain shift that had occurred after craniotomy. This registration takes five to ten minutes. A visual inspection of the data after registration (Figs. 4–5) showed that the MI-based registration of the preoperative MR with the intraoperative ultrasound, and thus the quantification of brain shift, was accurate for all patients. The results of the quantitative evaluation of the consistency of the MI-based registration approach are shown in Fig. 6. The average difference between the estimated shift from direct registration of the preoperative MR with the "post opening dura" intraoperative ultrasound, and the indirect measurement by registering twice, via "pre opening dura" ultrasound is 1.0 mm, with a maximum of 1.6 mm, which was significantly smaller than the magnitude of brain shifts that were observed.

In order to check if the mutual-information-based rigid registration improves the registration of the regions of interest, i.e., the tumors, the overlap of tumor tissue, segmented (in 3-D) in both the preoperative MR and the intraoperative ultrasound after opening the dura, was measured. After transforming the preop-

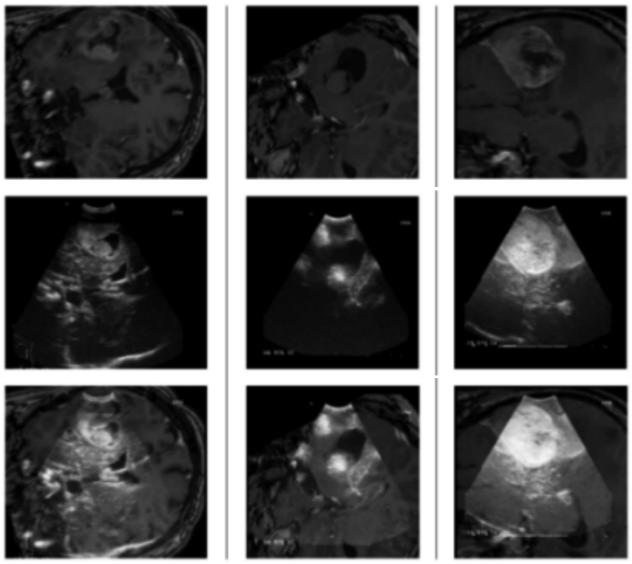

Fig. 5. MI-based registration of preoperative MR images and intraoperative US image, after opening the dura, prior to surgery for three patients. Upper row: MR images (registered with the MI-based method to US image), middle row: US images after opening the dura, bottom row: MR images with US overlay.

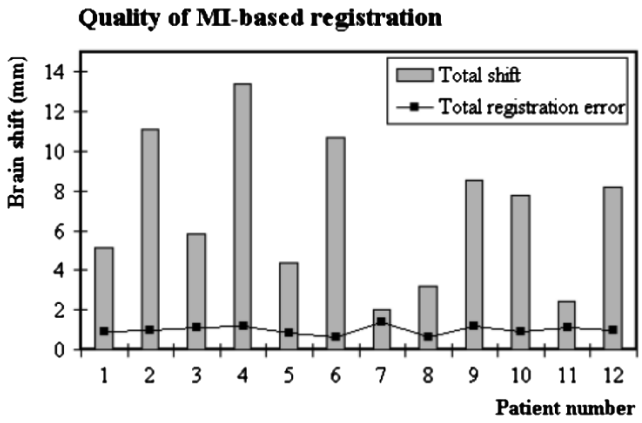

Fig. 6. Consistency check for the MI-based registration procedure for MR—ultrasound registration. The inconsistency of the MI-based registration procedure is measured by comparing a direct registration method of the preoperative MR to the "post opening dura" volume with an indirect registration method (from the preoperative MR volume via "pre opening dura" ultrasound volume, to "post opening dura" ultrasound volume). The inconsistency of the MI-based registration procedure was much smaller than the measured total shift, indicating that MI-based registration is a good method for registering MR and ultrasound images.

erative MR to the intraoperative ultrasound coordinate system, based on the rigid transformation provided by image-guided surgery system, the average volume overlap of tumor tissue was 72%. After MI-based rigid registration of the preoperative MR with the intraoperative ultrasound image the average volume overlap of tumor tissue increased to 83%.

Since the MI-based registration improves tumor overlap and is consistent, we use it as a basis for brain shift estimation. In Fig. 7, the brain shift parallel (left) and perpendicular (right) to gravity are shown. The shift is expressed as the number of millimeters the MR images has to be shifted to correlate with 1) the ultrasound image taken before opening the dura and 2) the ultrasound image taken after opening the dura. For the shift parallel to gravity a negative shift means sinking of the brain, while a positive shift means bulking of the brain. From Fig. 7 it can be seen that for 3 out of the 12 patients a bulking of the brain occurs prior to opening the dura, and for 4 out of the 12 patients a bulking of occurs after opening the dura. The parallel shift before opening the dura is on average 3.0 mm, with a maximum of 7.5 mm, and the perpendicular shift is 3.9 mm, with a maximum of 8.2 mm. After opening the dura the average parallel shift does not change much (0.2 mm) while the perpendicular shift is 1.4 mm larger. The maximum total brain shift measured, i.e., Euclidean distance, (Fig. 8) is 13.4 mm.

In Fig. 9, the main direction of this brain shift with respect to gravity is determined. The angle between the main direction of shift and gravity is on average 60°, with a maximum of 88°.

IV. Discussion

In this paper, we described the setup of an image-guided surgery system equipped with the additional functionality of intraoperative 3-D ultrasound imaging. Intraoperative imaging or updating is needed in image-guided surgery systems since brain shift occurs between the moment of preoperative (MR) imaging and the time of surgery. Since this brain shift can be up to 25 mm, it is one of the most limiting factors in the accuracy of image-guided surgery systems [3]–[7], [10]–[14].

We found that the brain tumors were well localized in the ultrasound data for all 12 patients. The tumor margins could be defined well in eight patients and moderately in four. This is consistent with findings of other researchers, who also found that intraoperative ultrasound can be helpful in localizing and defining margins of tumors, with the exception of some gliomas [32], [42], [47]–[49]. We also have shown that it is possible to transform the preoperatively acquired MR data in the coordinate system of the intraoperative 3-D ultrasound data, thus allowing an integrated display, visualizing the brain shift in 3-D.

To quantify the rigid component of brain shift, a rigid image registration method based on MI was used to register the MR data to the ultrasound data. A consistency check was performed by comparing a direct registration (from preoperative MR to intraoperative "post opening dura" ultrasound) with an indirect registration (from preoperative MR to intraoperative "post opening dura" ultrasound via intraoperative "pre opening dura" ultrasound; Fig. 6). The "consistency error" was considerably smaller than the observed brain shift and, therefore, the MI-based registration method is sufficiently consistent to accurately measure the rigid component of brain shift from the MR and ultrasound data.

The correctness of the estimated shift was also determined by checking whether tumor overlap increased after correction. We found the average overlap to be 72% after the rigid transformation given by the image-guided surgery system and 83% after MI-based rigid registration of the preoperative MR with the intraoperative ultrasound image. This means the MI-based registration did improve the overlap between the tumor segments, but the overlap does not approach 100%. There are three reasons for this nonperfect overlap. In an earlier study we found that, if

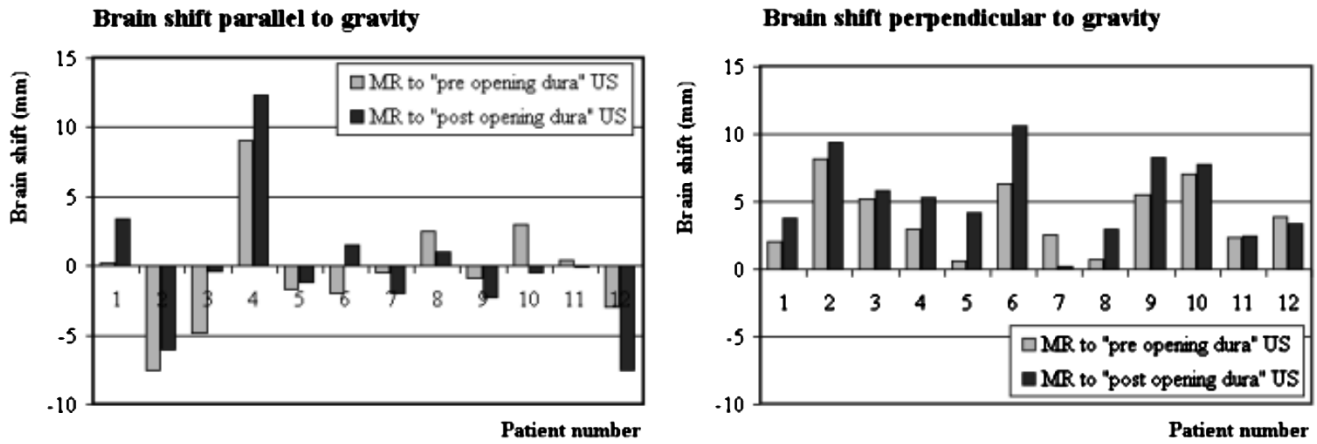

Fig. 7. Brain shift measured with an ultrasound probe, before and after opening the dura, with respect to the MR image taken prior to surgery. (left) Shift parallel to gravity. A positive shift indicates bulking of the brain, a negative shift indicates sinking of the brain. (right) Shift perpendicular to gravity. The perpendicular shift is indicated as an absolute value.

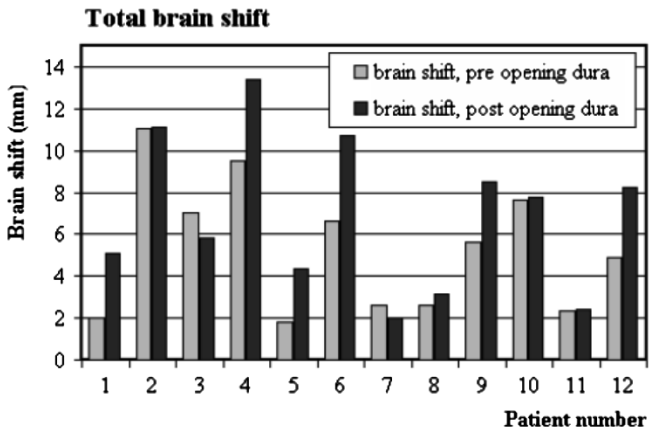

Fig. 8. Total brain shift measured, prior to opening the dura and after opening the dura.

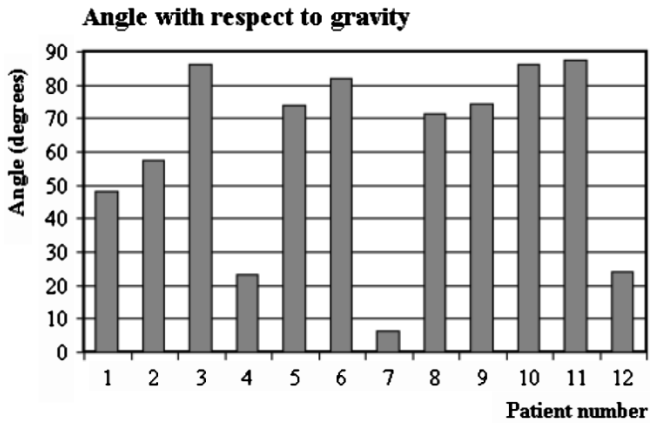

Fig. 9. The angle between the main direction of shift and the direction of gravity (after opening the dura).

two observers segment the same tumor, the average overlap between these two segmentations is about 90% [50]. Further the different image properties of MR and ultrasound images may lead to different definitions of the tumour border. The last likely reason for this nonperfect overlap is that the shift between the preoperative MR and the intraoperative ultrasound data can not be described by a rigid registration alone, nonrigid registration techniques are necessary to gain insight in the exact brain deformation that occurs.

Our main findings were that the rigid component of shift prior to opening the dura was on average 3.0 mm parallel to gravity and 3.9 mm perpendicular to gravity, while after opening the dura the shift was 3.2 mm parallel to gravity and 5.3 mm perpendicular to this. This means that, in our study, the shift from the moment of preoperative imaging to after craniotomy but before opening the dura is larger than the shift that is induced by opening the dura. The maximum shift measured was 13.4 mm. These results are consistent with earlier reported values [3]–[7], [10]–[14], of an average tumor shift of 3-7 mm with a maximum of 15 mm.

The shifts measured between the preoperative MR data and intraoperative ultrasound data can have two causes; a system registration error and a real brain shift. In order to estimate how much of the shift measured is actual brain shift the system registration error or system accuracy has to be discussed. For a thorough overview of all error sources that may influence the accuracy of a 3-D ultrasound-based neuronavigation system we refer to an article of Lindseth *et al.* [51]. Here, we will only discuss the main error sources.

The registration error from MR coordinates to arc coordinates can have different sources, e.g., slide of the skin fiducials, geometric distortions in the MR image, brain shift due to different positioning of the patient in OR with respect to the MR scan, errors in fiducial identification. All these error sources are expected to be small ($<$1 mm). The image-guided surgery we use has the ability to estimate this error by calculating how well the fiducials in the MR image can be matched to the fiducials on the patient, with aid of a least-square fitting method. Generally the registration error on the tumor surface is around 1 mm, and the error on the brain surface is around 1.5 mm. (The tumor position can be located more accurately since there are more fiducials located near the tumor). This error only affects the registration of the preoperative MR to the "pre opening dura" ultrasound scan.

The registration error from US coordinates to arc coordinates can also have different error sources, e.g., errors in the probe calibration, imperfect synchronization between the acquisition of the ultrasound B-scan and the corresponding position information, variations in the speed of sound, errors in the 3-D volume reconstruction of the B-scans. Of these errors the error in probe calibration is expected to have, by far, the largest influence on the accuracy [51]. We calculated this error to be 1.6 mm in the worst cases [52].

In our study we measured not only a sinking of the brain, but also a bulking of the brain. This means our results are different from the results of some authors who report only sinking of the brain [4], [10], [16], but others also report a clear bulking of the brain, which was also visible during surgery [3], [5], [13], [15].

Not only the amount of brain shift but also the direction of brain shift is important, since many biomechanical models assume that the brain is sinking in the direction of gravity after opening the dura. We measured the angle between gravity and the main direction of shift, which was on average 60° with a maximum of 88°, which is certainly not consistent with a main shift parallel to gravity. Based on our experience with 12 patients we hypothesize that the assumption of many biomechanical models is not correct and the brain does not simply sink with gravity, and that biomechanical modeling is much more complex than these assumptions.

One of the limitations of our study is that we used a relatively small patient group. Moreover, we only have an estimate for the gravity direction in our experiments. Studies on larger patient populations with explicit measurements of the orientation of the probe, and patient, with respect to gravity are planned. Furthermore, nonrigid registration methods will be evaluated in the future to gain more insight in the nature of brain deformations during surgery.

V. Conclusion

A system to acquire 3-D ultrasound data during image-guided neurosurgery has been described. By comparing 3-D ultrasound data to preoperative MR, the rigid component of brain shift could be measured. Therefore, the current setup can be used as a basis for correction for intraoperative brain deformations.

References

[1] T. M. Peters, "A Review of Image-guided surgery from X-rays to virtual reality," *Comput. Meth. Biomech. Biomed. Eng.*, vol. 4, no. 1, pp. 27–57, 2000.

[2] R. D. Bucholz, K. R. Smith, K. A. Laycock, and L. L. McDurmond, "Three-dimensional localization: From image-guided surgery to information-guided therapy," *Methods*, vol. 25, pp. 186–200, 2001.

[3] R. D. Bucholz, D. D. Yeh, J. Trobaugh, L. L. McDurmont, C. D. Sturm, C. Baumann, J. M. Henderson, A. Levy, and P. Kessman, "The correction of stereotactic inaccuracy caused by brain shift using an intraoperative ultrasound device," in *Lecture Notes in Computer Science*. Berlin, Germany: Springer-Verlag, 1997, vol. 1205, Proc. 1st Joint Conf. CVRMed and MRCAS, pp. 459–466.

[4] D. L. G. Hill, C. R. Maurer, R. J. Maciunas, J. A. Barwise, J. M. Fitzpatrick, and M. Y. Wang, "Measurement of intraoperative brain surface deformation under a craniotomy," *Neurosurgery*, vol. 43, no. 3, pp. 514–528, 1998.

[5] N. L. Dorwand, O. Alberti, B. Velani, B. Gerritsen, F. A. Harkness, W. F. Kitchen, and D. G. Thomas, "Postimaging brain distortion: Magnitude correlates and impact on neuronavigation," *Neurosurg. Focus*, vol. 10, no. 2, 2001. Article 3.

[6] R. M. Comeau, A. F. Sadikot, A. Fenster, and T. M. Peters, "Intraoperative ultrasound for guidance and tissue shift correction in image-guided neurosurgery," *Med. Phys.*, vol. 27, no. 4, pp. 787–800, 2000.

[7] G. J. Rubino, C. Lycette, K. Farahani, D. McGill, B. van de Wiele, and J. P. Villablanca, "Interventional magnetic resonance imaging guided neurosurgery—The UCLA experience with the first 100 cases," *Electromedica*, vol. 68, pp. 37–46, 2000.

[8] Medical Research Council Working Party, "Prognostic factors for high-grade malignant glioma: Development of a prognostic index—A report to the medical research council brain tumor working party," *J. Neurooncol.*, vol. 9, pp. 47–55, 1990.

[9] E. R. Laws, M. E. Shaffrey, A. Morris, and F. A. Anderson, "Surgical management of intracranial gliomas—Does radical resection improve outcome?," *Acta Neurochirurgica*, vol. Suppl. 85, pp. 47–53, 2002.

[10] D. G. L. Hill, C. R. Maurer, M. Y. Wang, R. J. Maciunas, J. A. Barwise, and J. M. Fitzpatrick, "Estimation of intraoperative brain surface movement," in *Lecture Notes in Computer Science*. Berlin, Germany: Springer-Verlag, 1997, vol. 1205, Proc. 1st Joint Conf. CVRMed and MRCAS, pp. 449–458.

[11] D. W. Roberts, A. Hartov, F. E. Kennedy, M. I. Miga, and K. D. Paulsen, "Intraoperative brain shift and deformation: A quantitative analysis of cortical displacement in 28 cases," *Neurosurgery*, vol. 43, no. 4, pp. 749–758, 1998.

[12] C. R. Maurer, D. L. G. Hill, A. J. Martin, H. Liu, M. McCue, D. Rueckert, D. Lloret, W. A. Hall, R. E. Maxwell, D. J. Hawkes, and C. L. Truwit, "Investigation of intraoperative brain deformation using a 1.5-T interventional MR system: Preliminary results," *IEEE Trans. Med. Imag.*, vol. 7, no. 5, pp. 817–825, Oct. 1998.

[13] H. Dickhaus, K. A. Ganser, A. Staubert, M. M. Bonsanto, C. R. Wirtz, V. M. Tronnier, and S. Kunze, "Quantification of brain shift effect by MR-imaging," in *Proc. 19th Annu. International Conf. IEEE Engineering in Medicine and Biology Society*, Chicago, IL, 1997, pp. 491–494.

[14] C. Nimsky, O. Ganslandt, S. Cerny, P. Hastreiter, G. Greiner, and R. Fahlbusch, "Quantification of, visualization of, and compensation for brain shift using intraoperative magnetic resonance imaging," *Neurosurgery*, vol. 47, no. 5, pp. 1070–1080, 2000.

[15] M. A. Audette and T. M. Peters, "Level-set surface segmentation and registration for computing intra-surgical deformation," *Proc. SPIE (Image Display)*, vol. 3661, pp. 110–121, 1999.

[16] M. I. Miga, K. D. Paulsen, J. M. Lemery, S. D. Eisner, A. Hartov, F. E. Kennedy, and D. W. Roberts, "Image guidance: Initial clinical experience with gravity-induced brain deformation," *IEEE Trans. Med. Imag.*, vol. 18, no. 10, pp. 866–874, Oct. 1999.

[17] D. W. Roberts, M. I. Miga, A. Hartov, S. Eisner, J. M. Lemery, F. E. Kennedy, and K. D. Paulsen, "Intraoperatively updated neuroimaging using brain modeling and sparse data," *Neurosurgery*, vol. 45, no. 5, pp. 1199–1207, 1999.

[18] K. D. Paulsen, M. I. Miga, F. E. Kennedy, P. J. Hoopes, A. Hartov, and D. W. Roberts, "A computational model for tracking subsurface tissue deformation during stereotactic neurosurgery," *IEEE Trans. Biomed. Eng.*, vol. 46, no. 2, pp. 213–225, Feb. 1999.

[19] O. Skrinjar, C. Studholme, A. Nabavi, and J. Duncan, "Steps toward a stereo-camera-guided biomechanical model of brain shift compensation," in *Proc. Information Processing in Medical Imaging (IPMI)*, Davis, CA, 2001, pp. 183–189.

[20] P. M. Black, T. Moriarty, E. Alexander, P. Stieg, E. J. Woodard, P. L. Gleason, C. H. Martin, R. Kikinis, R. B. Schwartz, and F. A. Jolesz, "Development and implementation of intraoperative magnetic resonance imaging and its neurosurgical applications," *Neurosurgery*, vol. 41, pp. 831–842, 1997.

[21] R. Steinmeier, R. Fahlbusch, O. Ganslandt, C. Nimsky, M. Buchfelder, M. Kaus, T. Heigl, G. Lenz, R. Kuth, and W. Huk, "Intraopertive magnetic resonance imaging with the magnetom open scanner: Concepts, neurosurgical indications and procedures: A preliminary report," *Neurosurgery*, vol. 43, pp. 739–748, 1998.

[22] J. J. van Vaals, "Interventional MR with a hybrid high-field system," in *Interventional Magnetic Resonance Imaging*, J. F. Debatin and G. Adam, Eds. Berlin, Germany: Springer-Verlag, 1998, pp. 19–32.

[23] H. Liu, W. A. Hall, and C. L. Truwit, "Neuronavigation in interventional MR imaging. Prospective stereotaxy," *Neuroimag. Clin. North Amer.*, vol. 11, no. 4, pp. 695–704, 2001.

[24] F. A. Jolesz, R. Kikinis, and I. F. Talis, "Neuronavigation in interventional MR imaging. Frameless stereotaxy," *Neuroimag. Clin. North Amer.*, vol. 11, no. 4, pp. 685–693, 2001.

[25] A. Hagemann, K. Rohr, H. S. Stiehl, U. Spetzger, and J. M. Gilsback, "Biomedical modeling of the human head for physically based, nonrigid image registration," *IEEE Trans. Med. Imag.*, vol. 18, no. 10, pp. 875–884, Oct. 1999.

[26] N. Hata, A. Nabavi, S. Wells, S. K. Warfield, R. Kikinis, P. McLBlack, and F. A. Jolesz, "Three-dimensional optical flow method for measurement of volumetric brain deformation from intraoperative MR images," *J. Comput. Assist. Tomogr.*, vol. 24, no. 4, pp. 531–538, 2000.

[27] M. Ferrant, A. Nabavi, B. Macq, F. A. Jolesz, R. Kikinis, and S. K. Warfield, "Registration of 3-D intraoperative MR images of the brain using a finite element biomechanical model," *IEEE Trans. Med. Imag.*, vol. 20, no. 12, pp. 1384–1397, Dec. 2001.

[28] T. Hartkens, D. L. G. Hill, A. D. Castellano-Smith, D. J. Hawkes, C. R. Maurer, A. J. Martin, W. A. Hall, H. Liu, and C. L. Truwit, "Measurement and analysis of brain deformation during neurosurgery," *IEEE Trans. Med. Imag.*, vol. 22, no. 1, pp. 82–92, Jan. 2003.

[29] J. M. Rubin, M. Mirfakhraee, E. E. Duda, G. J. Dohrmann, and F. Brown, "Intraoperative ultrasound examination of the brain," *Radiology*, vol. 137, pp. 831–832, 1980.

[30] J. W. Trobaugh, W. D. Richards, K. R. Smith, and R. D. Bucholz, "Frameless stereotactic ultrasonography: Methods and applications," *Computerized Med. Imag. Graphics*, vol. 18, pp. 235–246, 1994.

[31] J. Koivukangas, Y. Louhisalmi, J. Alakuijala, and J. Oikarinen, "Ultrasound-controlled neuronavigator-guided brain surgery," *J. Neurosurg.*, vol. 70, pp. 36–42, 1993.

[32] M. A. Hammoud, B. L. Ligon, R. elSouki, W. M. Shi, D. F. Schomer, and R. Sawaya, "Use of intraoperative ultrasound for localizing tumors and determining the extent of resection: A comparative study with magnetic resonance imaging," *J. Neurosurg.*, vol. 84, pp. 737–741, 1996.

[33] C. Giorgi and D. S. Casolino, "Preliminary clinical experience with intraoperative stereotactic ultrasound imaging," *Stereotactic Functional Neurosurg.*, pt. 1, vol. 68, no. 1–4, pp. 54–58, 1997.

[34] N. Hata, T. Dohi, H. Iseki, and K. Takakura, "Development of a frameless and armless stereotactic neuronavigation system with ultrasonographic registration," *Neurosurgery*, vol. 41, pp. 608–614, 1997.

[35] H. Hirschberg and G. Ungaard, "Incorporation of ultrasonic imaging in an optically coupled frameless stereotactic system," *Acta Neurochirurgica*, vol. Suppl. 68, pp. 74–89, 1997.

[36] G. E. Keles, K. R. Lamborn, and M. S. Berger, "Coregistration accuracy and detection of brain shift using intraoperative sononavigation during resection of hemispheric tumors," *Neurosurgery*, vol. 53, no. 3, pp. 556–564, 2003.

[37] G. Unsgaard, S. Ommedal, T. Muller, A. Gronningsaeter, and T. A. N. Hernes, "Neuronavigation by intraoperative three-dimensional ultrasound: Initial experience during brain tumor resections," *Neurosurgery*, vol. 50, pp. 804–812, 2002.

[38] A. Gronningsaeter, A. Kleven, S. Ommedal, T. E. Aarseth, T. Lie, F. Lindseth, T. Lango, and G. Unsgaard, "Sonowand, an ultrasound-based neuronavigation system," *Neurosurgery*, vol. 47, no. 6, pp. 1373–1380, 2000.

[39] A. N. Hernes, S. Ommedal, T. E. Aarseth, T. Lie, F. Lindseth, T. Lango, and G. Unsgaard, "Stereoscopic navigation-controlled display of preoperative MRI and intraoperative 3D ultrasound in planning and guidance of neurosurgery: New technology for minimally invasive image-guided surgery approaches," *Minimally Invasive Neurosurg.*, vol. 46, no. 3, pp. 129–137, 2003.

[40] A. Jödicke, W. Deinsberger, H. Erbe, A. Krieter, and D. K. Böker, "Intraoperative three-dimensional ultrasonography: An approach to register brain shift using multidimensional image processing," *Minimally Invasive Neurosurg.*, vol. 42, pp. 13–19, 1998.

[41] D. G. Gobbi and T. M. Peters, "Interactive intra-operative 3D ultrasound reconstruction and visualization," in *Lecture Notes in Computer Science*, T. Dohi and R. Kikinis, Eds, Berlin, Germany: Springer-Verlag, 2002, vol. 2489, Proc. MICCAI, pp. 156–163.

[42] V. M. Tronnier, M. M. Bonsanto, A. Staubert, M. Knauth, S. Kunze, and C. R. Wirtz, "Comparison of intraoperative MR imaging and 3D-navigated ultrasonography in the detection and resection control of lesions," *Neurosurg. Focus*, vol. 10, no. 2, 2001. Article 3.

[43] C. Trantakis, J. Meixensberger, D. Lindner, G. Strauss, G. Grunst, A. Schmidtgen, and A. Arnold, "Iterative neuronavigation using 3D ultrasound. A feasibility study," *Neurological Res.*, vol. 24, no. 6, pp. 666–670, 2002.

[44] L. G. Bouchet, S. L. Meeks, G. Goodchild, F. J. Bova, J. M. Buatti, and W. A. Friedman, "Calibration of three-dimensional ultrasound images for image-guided radiation therapy," *Phys. Med. Biol.*, vol. 46, pp. 559–577, 2001.

[45] R. W. Prager, A. Gee, and L. Berman, "StradX: Real-time acquisition and visualization of freehand three-dimensional ultrasound," *Med. Image Anal.*, vol. 3, no. 2, pp. 129–140, 1999.

[46] P. Perona and J. Malik, "Scale-space and edge detection using anisotropic diffusion," *IEEE Trans. Pattern Anal. Machine Intell.*, vol. 12, no. 7, Jul. 1990.

[47] L. M. Auer and V. van Velthoven, "Intraoperative ultrasound imaging. Comparison of pathomorphological findings in US and CT," *Acta Neurochirurgica*, vol. 104, pp. 84–95, 1990.

[48] P. D. LeRoux, M. S. Berger, and K. Wang, "Low grade gliomas: Comparison of intraoperative ultrasound characteristics with preoperative imaging studies," *J. Neurooncol.*, vol. 13, pp. 189–198, 1992.

[49] V. van Velthoven, "Intraoperative ultrasound imaging: Comparison of pathomorphological findings in US versus CT, MRI, and intraoperative findings," *Acta Neurochirurgica*, vol. Suppl. 85, pp. 95–99, 2002.

[50] M. M. J. Letteboer, W. J. Niessen, P. W. A. Willems, E. B. Dam, and M. A. Viergever, "Interactive multi-scale watershed segmentation of tumors in MR brain images," in *Proc. Interactive Medical Image Visualization and Analysis*, S. D. Olabarriaga, W. J. Niessen, and F. A. Gerritsen, Eds., 2001, pp. 11–16.

[51] F. Lindseth, T. Lango, J. Bang, and T. A. N. Hernes, "Accuracy evaluation of a 3D ultrasound-based neuronavigation system," *Comput. Aided Surg.*, vol. 7, pp. 197–122, 2002.

[52] F. Rousseau, M. M. J. Letteboer, P. Hellier, W. J. Niessen, and C. Barillot, Quantitative evaluation of calibration methods for 3D freehand ultrasound, 2005, submitted for publication.

Marloes M. J. Letteboer, photograph and biography not available at the time of publication.

Peter W. A. Willems, photograph and biography not available at the time of publication

Max A. Viergever (M'99), photograph and biography not available at the time of publication

Wiro J. Niessen (S'94–A'97), photograph and biography not available at the time of publication